

Carbon and nitrogen Isotope fractionation of the photo-degradation of herbicides in aqueous solution by nitrates under ultraviolet radiation

Haiyan Yu

Tongji University College of Environmental Science and Engineering

Jinling Liu

Tongji University College of Environmental Science and Engineering

Changxu Han

Tongji University College of Environmental Science and Engineering

Han Fang

Tongji University College of Environmental Science and Engineering

Xingquan Shu

Tongji University College of Environmental Science and Engineering

Yongfeng Liu

Tongji University College of Environmental Science and Engineering

Yuwei Pan

Nanjing Forestry University

Limin Ma (✉ Imma@tongji.edu.cn)

Tongji University College of Environmental Science and Engineering <https://orcid.org/0000-0002-3819-2111>

Research

Keywords: Herbicides, Photodegradation, CSIA, Isotope fractionation

Posted Date: January 7th, 2020

DOI: <https://doi.org/10.21203/rs.2.20182/v1>

License: © ⓘ This work is licensed under a Creative Commons Attribution 4.0 International License.

[Read Full License](#)

1 **Carbon and nitrogen Isotope fractionation of the photo-**
2 **degradation of herbicides in aqueous solution by nitrates**
3 **under ultraviolet radiation**

4 Haiyan Yu^a, Jinling Liu^a, Changxu Han^a, Han Fang^a, Xingquan Shu^a, Yongfeng Liu^a,
5 Yuwei Pan^b, Limin Ma^{ac*}

6 ^a College of Environmental Science and Engineering, Tongji University, Shanghai 200092, China

7 ^b College of Biology and the Environment, Nanjing Forestry University, Nanjing 210037, China

8 ^c Shanghai Institute of Pollution Control and Ecological Security, Shanghai 200092, China

9

10

11

12

13

14 *** Corresponding author at:** College of Environmental Science and Engineering,
15 Tongji University, Shanghai 200092, China.

16 **E-mail address:** lmma@tongji.edu.cn.

17

18

19

20

*** Corresponding author at:** College of Environmental Science and Engineering, Tongji University, Shanghai 200092, China
E-mail address: lmma@tongji.edu.cn

21 **Abstract**

22 **Background:** Phenylurea herbicides are one of the most important and widely used
23 pesticides in the world. Due to its potential persistence and toxicity in the aquatic
24 environment, it poses certain risks to the ecological environment and human health.
25 Studying the photochemical degradation behavior of herbicides is important for
26 understanding the degradation and transformation fate in the environment.

27 **Results:** This study evaluated the effectiveness of direct and indirect photo-degradation
28 of the herbicides isopropiron (IUP) and methylamine (MN), investigating the influence
29 of operational variables (initial herbicide concentration and light sources) and initial of
30 induced nitrate concentration on these processes in aqueous solution. We also
31 introduced a new technology of compound-specific isotope analysis (CSIA) to provide
32 deeper information of the photochemical degradation mechanism. Results showed that
33 the light source and the initial concentration have an important effect on the degradation
34 of herbicides IUP and MN. The photolysis rate under the Hg lamp is higher than
35 photolysis rate under Xe lamp. It is found that photolysis kinetics of herbicides were
36 consistent with the quasi-first order model, and the photolysis rate decreases with the
37 increasing of the initial concentration. In indirect photodegradation, the degradation
38 rate increases with increasing NO_3^- concentration at low concentrations of pesticides (8
39 mg/L); while the degradation rate decreases with increasing NO_3^- concentration at high
40 concentrations of pesticides (30 mg/L). According to the isotope fractionation,
41 photolysis of IUP exhibits normal carbon isotope fractionation with the degradation rate
42 increases, and the stable isotope enrichment factors under different photolysis pathways

43 are different. In the indirect photo-degradation process, no significant fractionation of
44 nitrogen isotopes occurred, and stable nitrogen isotopes fractionation could not be fitted
45 well in either of the two photodegradation pathways.

46 **Conclusion:** Therefore, the structure and chemical characteristics of the molecules of
47 herbicides play a determinant role in their photodegradation. The CSIA is useful both
48 for a mechanism-based evaluation of experimental results and as a valuable tool to
49 explore transformation pathways for organic pollutants in different environmental
50 systems.

51
52 **Keywords:** Herbicides; Photodegradation; CSIA; Isotope fractionation

53

54

55 **Background**

56 Environmental contamination by pesticides is an issue of general concern since
57 these compounds can adversely affect human and ecosystem health, due to the highly
58 toxic, carcinogenic, and biological pollutants with a long-term residual nature [1-4]. In
59 response to the rapid development of agriculture in recent years, herbicides are widely
60 used to achieve maximum crop yields [4, 5]. Since the 1990s, the application amount
61 of pesticide in China has been on a rapid rise, increasing to 1.8 million tons in 2013,
62 with an average annual growth rate of 7.4% [6]. Most pesticides can be discharged from
63 agricultural activities, industrial wastewater, dispersed through evaporation into the air,
64 attached to plants, or leached into groundwater, leading to greater serious chemical
65 pollution in the water and soil environment [1, 5, 7]. The pesticide residue concern has

66 increased significantly, the government and scientists have made tremendous efforts in
67 detecting, monitoring, and degradation of the various pesticides residue in the
68 environment over the past several years [2, 8, 9]. Pesticide degradation includes both
69 microbial or plant-mediated biotransformation processes, as well as non-biological
70 processes such as chemical and photochemical reactions [10-12]. The transformation
71 process of a pesticide depends on its structural affinity for a particular type of
72 transformation and the environmental conditions to which its distribution and
73 transportation behavior is exposed [5, 13]. The resistance of some compounds to
74 conventional treatments has led to the application of other methods, such as photo-
75 oxidation which apply the radiant energy to the system, which generates electronically
76 excited molecules in different states. These molecules can be split, split, or
77 photoionized. In addition, the absorption of light in the visible or ultraviolet radiation
78 range can change the internal energy of the molecules, creating electronic transitions
79 between the molecules [5, 14].

80 Light-induced organic pollutants degradation (direct or indirect photolysis), is an
81 important degradation pathway for removing pesticides such as pesticides and
82 herbicides on surface water, soil and plant surfaces [15-18]. It has been reported that
83 ultraviolet (UV) radiation is considered as an alternative technology for removing
84 organic pollutants, owing to its high efficiency in removing certain pesticides and drugs
85 from water [19-23]. Most herbicides are photosensitive because their structures include
86 aromatic rings, heteroatoms, and other functional groups that make them susceptible to
87 UV radiation absorption (direct photolysis), or with photo-degradation that can induce

88 herbicides in water of light-sensitive species (indirect photolysis) [5, 23]. There have
89 been various studies on the use of direct and indirect UV photolysis to remove
90 herbicides from water [12, 21, 22, 24, 25]. Significant advances have recently been
91 made in our understanding of the photochemical processes undergone by organic
92 contaminants and pharmaceuticals in aqueous medium [26-30]. Some of these studies
93 have reported the indirect photodegradation by heterogeneous TiO₂ photocatalysis [31,
94 32], determined by the photo-induced by Fe(III) in aqueous solutions [33] and the
95 generation of situ hydroxyl radicals ([•]OH) [34]. It have been reported that nitrates
96 (NO₃⁻) is inorganic ions present in natural waters and can also induce the
97 photodegradation of phenylureas [35, 36]. The photochemistry of NO₃⁻ ions in aerated
98 aqueous solutions contains two main processes: the first yields [•]NO₂ and [•]OH, and the
99 second yields NO₂⁻ and O(³P) [37-39]. The assessment of the fate of these chemicals in
100 the environment requires knowledge and information on their degradation pathways
101 [40]. However, there has been little information on the use of these methods to treat
102 other pesticides widely used in agriculture, e.g., substituted phenylureas as a group of
103 herbicides widely used for general weed control of non-crop area and as pre-emergence
104 treatment on cereals and vegetable crops [41], despite their frequent detection in ground,
105 surface, and even tap waters [5, 42]. Furthermore, the conventional approach based on
106 concentration measurements of parent compounds and transformation products are not
107 conclusive, since a decrease of concentration might also be caused by dilution, sorption
108 and further transformation of metabolites [43-46]. Physical processes such as dilution,
109 diffusion, and volatilization almost do not change the isotope compositions to the same

110 extent as chemical or biochemical processes such as degradation [43, 44, 47, 48].
111 Compound-specific isotope analysis (CSIA) is a helpful analytical method for
112 characterizing the (bio)chemical transformation of organic contaminants based on
113 kinetic isotope effects during unidirectional reaction processes [40, 49-51]. Over recent
114 years, the method has become an increasingly valuable tool to assess the origin and fate
115 of organic contaminants in the environment [52-55]. CSIA may identify and quantify
116 transformation reactions of organic contaminants [56-58]. To date, there is little
117 information on the photolysis of organic pollutants associated with CSIA.

118 Based on these backgrounds, the purpose of the present study are (1) investigate
119 the effectiveness and importance of UV radiation on the direct photo-degradation and
120 the nitrate-induced photo-degradation process on isopropiron (IUP) and methylamine
121 (MN) in aquatic mesocosms; (2) explore the influence of different operational variables
122 (initial herbicide concentration and nitrate concentration) during photodegradation of
123 the herbicides; (3) apply the CSIA to further investigate the reactivity and
124 photodegradation of IUP, providing a theoretical basis for comprehensive
125 understanding of the photolysis and degradation characteristics of herbicides and
126 evaluating their behavior and safety in water environment.

127 **Materials and methods**

128 **Chemicals**

129 IUP (purity $\geq 99\%$) and MN (purity $\geq 98.5\%$) were analytical reagent grade and
130 supplied by Zhongshan Chemical Co., Ltd. HPLC grade organic solvents such as
131 methyl alcohol, acetonitrile, acetone and other chemical reagents were purchased from

132 ANPEL Scientific Instrument (Shanghai) Co., Ltd.

133 **Photodegradation experiments**

134 All herbicide degradation experiments were conducted in Rotary
135 photodegradation reactor. The light source is placed in a cold trap inside the double-
136 layer quartz, and the external cooling circulating water is used to reduce the temperature
137 of the lamp tube and filter out most of the infrared heat. The reaction temperature of the
138 dark box is maintained at 25 °C. Before each photodegradation experiment, the light
139 source is preheated. After 20 minutes of stabilization, a photodegradation experiment
140 was performed. In each experiment, after stabilizing the lamp and controlling the
141 temperature (25 °C), the photoreactor was turned on, and aliquots were drawn from the
142 reactor at different time intervals in order to assess the herbicide concentration. In the
143 direct photodegradation experiments, there are two different light sources in the cold
144 trap: high-pressure mercury lamp (main wavelength 365 nm, 500 W) and simulated
145 natural light long arc xenon lamp (300 ~ 800 nm, 500 W). While in the nitrate induced
146 degradation experiments, all reserve fluids were prepared with ultra-pure water to
147 exclude the quenching effect of organic solvents such as methanol on the instantaneous
148 photoactive product-OH. Further experiments focused on investigating: (1) the
149 influence of different light sources (Hg lamp and Xe lamp) on the concentrations of
150 IUP and MN (20 mg/L) photodegradation; (2) the influence of IUP and MN initial
151 concentrations (6, 12, and 25 mg/L) under the irradiation of Hg lamp; (3) the effect of
152 NO₃⁻ concentration (0, 0.5, 1, and 5 mM) under herbicides concentration of 8 and 30
153 mg/L; (4) the influence of herbicides concentrations (8, 15, and 20 mg/L) under a fixed

154 NO₃⁻ concentration of 5 mM. Control tests in the absence of nitrate induced under
155 different conditions were conducted in parallel.

156 **Chemical analysis**

157 Aqueous herbicide samples were filtered and then measured using a HPLC-DAD
158 system (LC-A10 series system, Shimadzu, Japan) and separation was conducted by an
159 ACE Excle 5 C₁₈-AR column (5 μm, 250×4.6mm, Advanced Chromatography
160 Technologies Ltd.). The mobile phase was acetonitrile/water for IUP (70 : 30, v/v) and
161 MN (60 : 40, v/v), at a flow rate of 1 mL/min and the herbicides were detected and
162 quantified at a wavelength of 245 nm.

163 **Compound-specific stable isotope analysis for carbon by GC-IRMS**

164 Sample preparation and isotope analysis were adapted from methods reported by
165 Meyer et al. [59]. The GC-IRMS system consists of TRACE GC Ultra gas
166 chromatograph (Thermo Fisher Scientific) equipped with a Trace Gold analytical
167 column (30 m×0.25 mm×0.25 μm), which was coupled to a Finnigan MAT 253 isotope
168 ratio mass spectrometer (IRMS) via a Finnigan GC Combustion III interface (Thermo
169 Fisher Scientific). Liquid samples were injected with a GC Pal auto sampler. The GC
170 oven temperature started at 40 °C (hold 5min) and consequently increased to 100°C
171 (hold 5 min) at rate of 50 °C/min. Then at a ramp of 15 °C/min consequently increased
172 to 300 °C (hold 5 min). During isotope analysis by GC-IRMS, analytes were measured
173 against a laboratory standard gas, which was introduced into at the beginning and the
174 end of each run. Both standard gases were calibrated to Vienna Pee Dee Belemnite (V-
175 PDB) and Air, respectively. Isotope values of carbon and nitrogen was reported as δ¹³C

176 and $\delta^{15}\text{N}$ values in ‰ relative to Vienna Pee Dee Belemnite (VPDB) according to eq.

177 (1) [60]:

$$178 \quad \delta^{13}E = \frac{R_{\text{sample}} - R_{\text{reference}}}{R_{\text{reference}}} \times 1000 \quad (1)$$

179 where R_{sample} and $R_{\text{reference}}$ are isotope ratios of the elements of concern in the
180 target compound and the international reference standard (e.g., VPDB for the carbon
181 isotope), respectively.

182 The changes in bulk isotope ratios of target compounds can be directly related to
183 the degradation progress by the enrichment factor (ϵ) following the Rayleigh equation
184 (eq. (2)) [61]:

$$185 \quad \ln\left(\frac{R_t}{R_0}\right) = \epsilon \times \ln\left(\frac{c_t}{c_0}\right) = \epsilon \times \ln(f) \quad (2)$$

186 where R_t and R_0 are the stable isotope ratios of the elements of concern in the molecules
187 of the target compounds at reaction time t and the beginning of degradation. f is the
188 remaining fraction of target compounds in the reaction pool.

189 **Results and discussion**

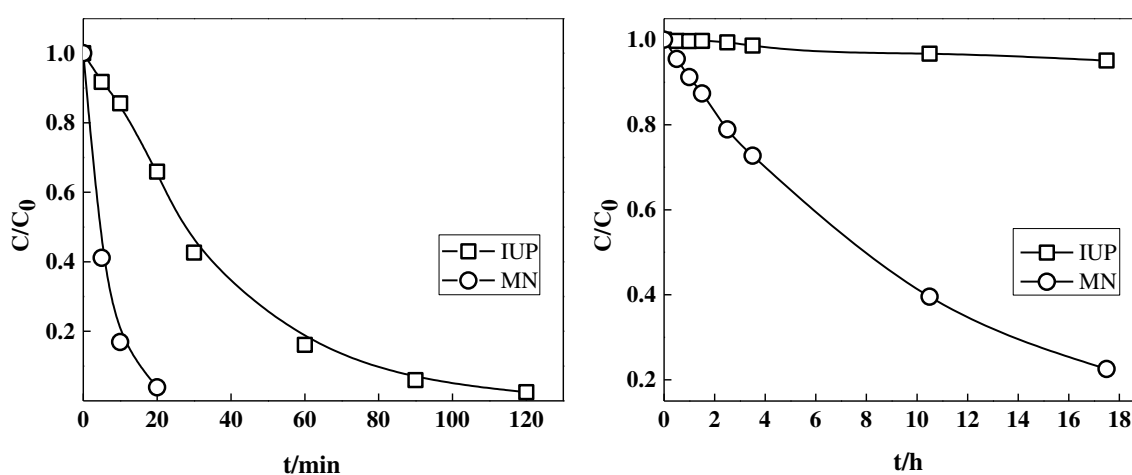
190 **The factors affecting photodegradation of herbicides**

191 **Effects of light sources kinetics of herbicides photochemical reaction**

192 The photodegradation of IUP and MN with concentrations at 20 mg/L under high
193 pressure Hg lamp and Xe lamp were investigated, and the results are shown in Fig. 1.
194 As shown in Fig. 1, no obvious degradation of IUP and MN was observed in dark
195 controls. The degradation rate of MN reached 99% within 60 min and IPU reached 99%
196 within 120 min under the condition of Hg lamp. Meanwhile, the degradation rate of
197 each organic pesticide significantly decreased, when the irradiation time reached 18 h,

198 the MN degradation rate was 78%, while the degradation rate of IPU was only 5% under
 199 the condition of Xe lamp. The extremely low light absorption of IUP and MN at
 200 wavelengths >290 nm is the reason for its persistence to photo-degradation [62]. In the
 201 natural environment, the emission wavelength of sunlight reaching the ground is mainly
 202 above 290 nm, while those less than 290 nm are absorbed by the ozone layer. Therefore,
 203 ultraviolet light at 290 nm \sim 450 nm is an important factor for the photodegradation of
 204 organic pesticides in the natural environment. Experiment of high pressure mercury
 205 lamp within 290 \sim 450 nm wavelength distribution (emission wavelength are centered
 206 around 360 nm), and maximum absorption spectrum of organic pesticide height weight
 207 stack with isopropyl lung and destroy the grass long because both belong to the benzene
 208 urea herbicide (functional groups $-\text{CH}(\text{CH}_3)_2$, its absorption spectrums are similar, there
 209 are two strong suction wave period, points don't in the left right around 240 nm and 210
 210 nm.

211



212

213 **Fig. 1.** Removal kinetics of herbicides by ultraviolet photodegradation. Notes: “a” presents Hg

214 lamp, “b” presents Xe lamp.

215 The linearized pseudo-first order kinetic model of IUP and MN under different
216 light conditions and the assessed parameters are presented in Table S1. According to
217 the fitting correlation coefficient (r^2), the pseudo-first order kinetic model exhibited
218 good consistency with experimental data and could describe the dynamic processes of
219 photodegradation. Under the two light sources, the photodegradation rate of the two
220 organic pesticides presented the same rule, and the degradation rate was $MN > IPU$.
221 Among them, MN degrades the fastest, and the half-life of Hg lamp and Xe lamp were
222 about 4 min and 8 h, respectively. IPU descending solution is the slowest, with half-life
223 of 22 min and 239 h, respectively.

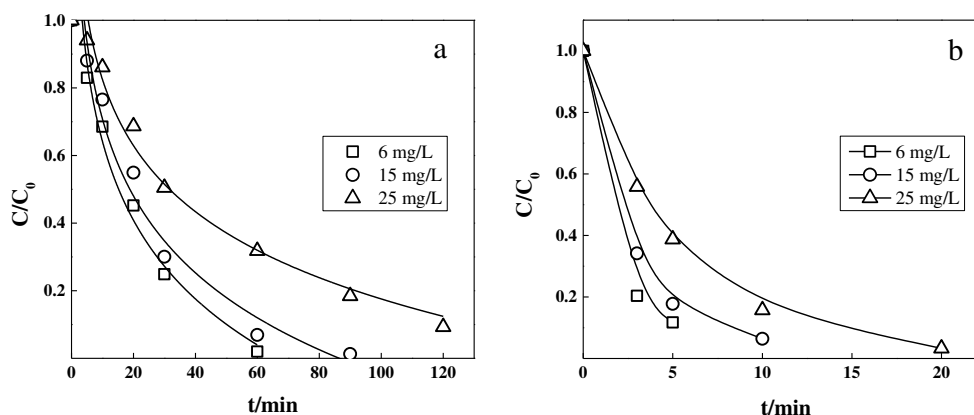
224 It's well known that the photodegradation rate of organic pesticides is related to
225 environmental factors (pH, temperature, and light source, etc.) [63], as well as its
226 structure [64]. The photolysis rate varies with the absorbance of different molecular
227 structures. According to the photolysis reactions of IPU and MN, the biggest difference
228 is that the IPU is demethylated, while the first reaction for MN is the dehalogen reaction.
229 In terms of the electron effect, MN as the chlorinated heterocyclic organic compounds,
230 since chlorine atom Cl (halogen atom) belongs to a strong electron-withdrawing group,
231 the electron cloud density on the heterocyclic ring decreases, and the C-Cl bond is very
232 easy to break through the isomerism mechanism. The $-CH(CH_3)_2$ at the end of the
233 aromatic ring of IPU belongs to the electron-donating group, and the electron cloud
234 density on the aromatic ring increases. Therefore, under the same light source, the
235 degradation of IPU requires more radiation energy and slower degradation rate.
236 Furthermore, from the absorption scanning spectrum of organic pesticides themselves,

237 MN has two strong absorption bands in the ultraviolet region, so it is highly active and
238 easy to absorb light radiation energy, leading to faster degradation. In addition, the
239 photo-degradation rate of organic pesticides is also related to the spatial structure of
240 parent molecules. Direct photolysis of MN is mainly through aromatic/heterocyclic
241 dechlorination of Cl and hydroxylation, which will undergo a series of free radical
242 reactions after being photoexcited. It has been reported that the shorter the chain length,
243 the more compact the molecular space structure, and the lower the degradation rate [5].

244 **Effect of initial concentration of IPU and MN**

245 The effect of initial concentration of IPU and MN were examined with different
246 concentrations at 6, 12, and 25 mg/L under the irradiation of Hg lamp (Fig. 2 and Table
247 S2). As shown in Fig. 2, with the increasing of initial concentration of herbicides, the
248 degradations were decreased. It indicates that initial concentration greatly affects the
249 degradation of IPU and MN. When initial concentration was 6 mg/L, the degradation
250 rate constant was 0.654 min^{-1} , and IPU was degraded completely within 60 min.
251 However, when the initial concentration was increased to 25 mg/L, degradation rate
252 constant was decreased to 0.0199 min^{-1} , complete degradation of which needed more
253 than 120 min. It might be the reason that degradation amount of atrazine is affected by
254 light intensity [65]. Therefore, under invariable light intensity, the degradation rate of
255 atrazine decreases when the concentration of IPU and MN in the aqueous solution is
256 increased. The degradation followed a first order rate equation, which is confirmed by
257 the evidence of a straight line relationship of logarithmic IPU and MN concentration
258 versus irradiation time ($r^2 > 0.9$), which is similar to other researches [65, 66].

259



260

261 **Fig. 2.** Influence of the initial concentration of herbicides on the photodegradation. Notes: “a”

262 presents IUP, “b” presents MN.

263

264 **Photo-degradation induced by nitrate ions**

265 **Effect of nitrate concentration**

266 In order to explore the effect of NO_3^- concentration, degradation of IPU and MN

267 (8 mg/L and 30 mg/L) in the presence of different NO_3^- concentration was carried

268 out. The results of these experiments are shown in Fig. 3 and Fig. 4. The linearized

269 pseudo-first order kinetic model of IPU and MN degradation and the assessed

270 parameters are presented in Table S3. The transformation of IPU and MN followed

271 pseudo-first order kinetics in the NO_3^- degradation system ($r^2 > 0.9$), and the presence

272 of NO_3^- has a photosensitizing effect on IPU and MN. Fig. 3 and Fig. 4 shows the

273 experimental result when the same concentration of IPU and MN (8 mg/L) was

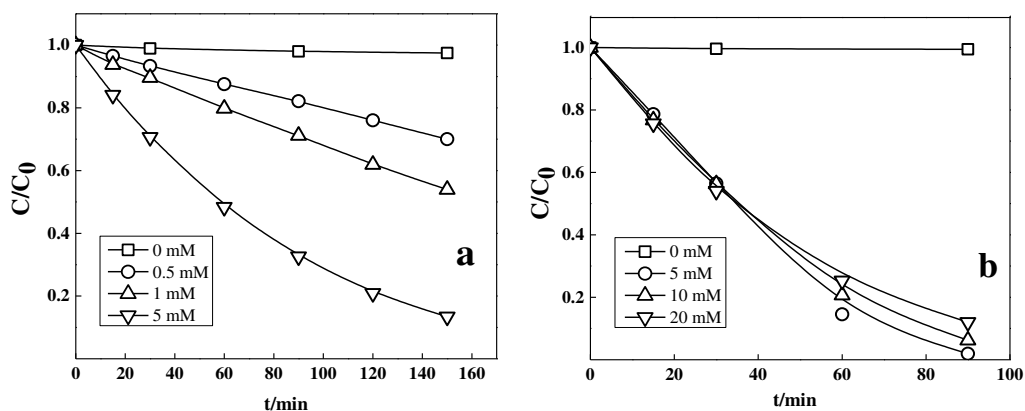
274 conducted with different concentration at 0, 0.5, 1 and 5 mM. It was obvious that nitrate

275 induction can significantly affect the degradation rate of organic pollutants, which is

276 consistent with the research results of Shankar et al. [35]. The experiment with low

277 concentration of the IUP (8 mg/L), the degradation rate increased with the increase of
 278 NO_3^- concentration. The result was directly linked to the production rates of the $\cdot\text{OH}$
 279 radical reactive species and constituted the main active species generated after
 280 irradiation [39]. However, at a higher concentration level (30 mg/L), the degradation
 281 rate decreased with the increase of NO_3^- concentration. It might be the reason that when
 282 the concentration of NO_3^- increases, NO_2^- as a quencher of $\cdot\text{OH}$ starts to limit the
 283 reaction of $\cdot\text{OH}$ with organic substrates, resulting in an increase in NO_3^- with a linear
 284 relationship with the generated $\cdot\text{OH}$; meanwhile, since the light intensity irradiated into
 285 the solution is a certain value, when the NO_3^- concentration increases, the unit of light
 286 energy received by NO_3^- decreases, and the excited NO_3^- by irradiation decreases, so
 287 the $\cdot\text{OH}$ produced decrease [65, 67], resulting in the degradation rate of the organic
 288 matrix decreases with increasing NO_3^- concentration. It's worth noting that there is no
 289 obvious degradation was found in the control group in the light solution without NO_3^-
 290 for IUP, indicating that the presence of NO_3^- was the main cause of herbicide
 291 degradation under light conditions.

292



293

294 **Fig. 3.** Influence of the nitrate concentration on the photodegradation of IUP by UV radiation. Notes:

295 “a” presents substrate concentration is 8 mg/L, “b” presents substrate concentration is 30 mg/L.

296

297 It’s worth noting that the photodegradation rate of MN was higher than that of IUP.

298 However, with the increase of NO_3^- concentration, the degradation rate ratio of IUP was

299 significantly greater than that of MN with the same NO_3^- concentration. When the NO_3^-

300 concentration was increased to 5 mM, the ratio of photo-degradation rate of IUP to its

301 single light exposure was 12.3 times, while the ratio of photodegradation rate of MN to

302 its single light exposure was 4 times, suggesting that IUP was more easily degraded

303 under the induction of NO_3^- due to the activity of alkyl on -OH and the deactivation of

304 electron-absorbing group halogen (-Cl) by electrophilic attack [35, 68]. In addition, we

305 found that although both IUP and MN belong to the phenylurea herbicides, their photo-

306 degradation promotion under NO_3^- induced is completely different, indicating that the

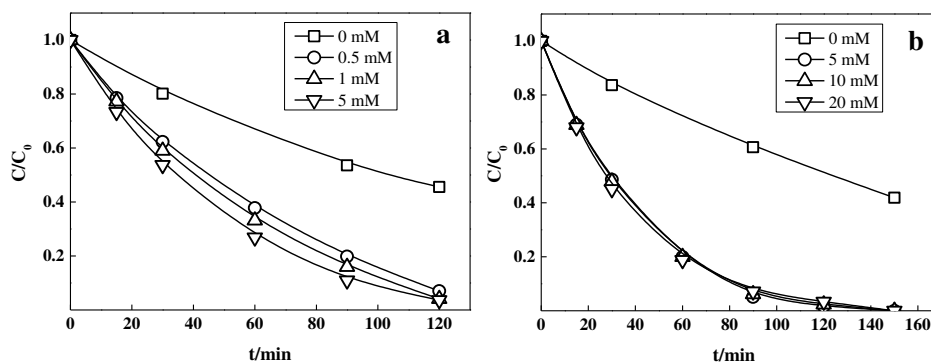
307 structure and chemical characteristics of herbicide molecules played a decisive role in

308 photo-degradation [5]. Hence, after initiation of the degradation process (a stage that is

309 closely related to the herbicide quantum yield), the degradation rate depends on the

310 lability of molecules faced by the attack of the radicals that are formed [5].

311



312

313 **Fig. 4.** Influence of the nitrate concentration on the photodegradation of MN by UV radiation. Notes:

314 “a” presents the substrate concentration is 8 mg/L, “b” presents the substrate concentration is 30
315 mg/L.

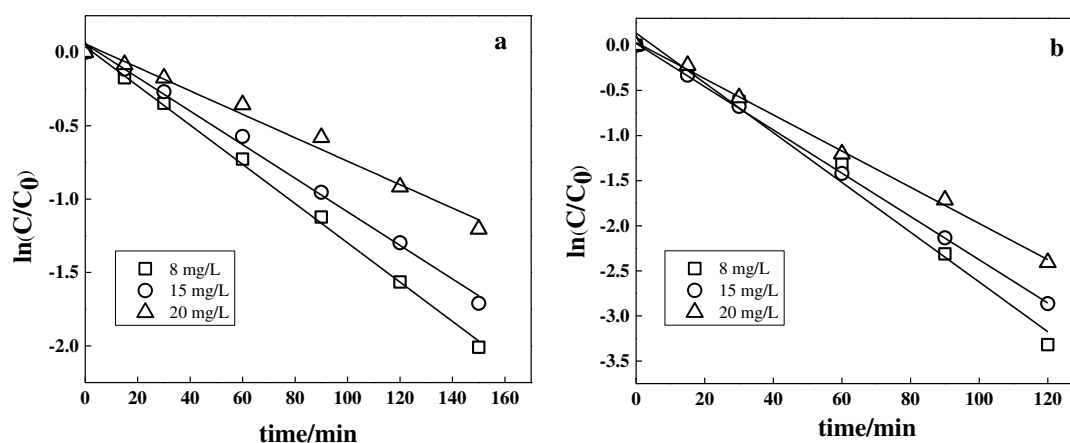
316

317 **Effect of substrate concentration**

318 To explore the influence of substrate concentration on the photodegradation rate
319 was studied at different concentrations (8, 15, 20 mg/L) with a certain concentration of
320 NO_3^- as the photoinducer (5 mM), and the results are shown in Fig. 5 and Table S4. The
321 photodegradation reactions followed pseudo-first order kinetics and the k_{obs} values that
322 were obtained clearly depended on the substrate concentration. The substrate
323 concentration increased from 8 mg/L to 20 mg/L, the degradation rate of IUP decreased
324 from 0.0222 min^{-1} to 0.019 min^{-1} , and the degradation rate of MN decreased from
325 0.0272 min^{-1} to 0.0228 min^{-1} . It was found that the photodegradation rate decreased
326 with the increase of organic substrate concentration with a certain concentration of
327 NO_3^- , which could be explained by competitive absorption between nitrate and
328 herbicides [39]. Therefore, an indirect reduction in $\cdot\text{OH}$ radicals (screen effect) or the
329 production of $\cdot\text{OH}$ was not in excess compared to the organic pollutants molecules [41].
330 With the concentration of the organic substrate increasing, the number of organic
331 substrate molecules per unit volume is increased, and the amount of $\cdot\text{OH}$ produced by
332 NO_3^- is constant, resulting in a decrease in the degradation rate of the matrix. Another
333 important reason is that with the organic substrate concentration increasing, it absorbs
334 light energy in a competitive relationship with the nitrate, resulting in $\cdot\text{OH}$ becoming
335 the rate control step [41]. These results were the same as that of Nelieu et al. and Hadjira

336 Boucheloukh et al. [39, 41], the increase in substrate concentration leads to an indirect
337 decrease in OH, and the amount of OH produced is not sufficient to react with organic
338 substrates.

339



340

341 **Fig. 5.** Influence of the substrate concentration on the photodegradation in the presence of NO_3^- (5
342 mM). Notes: “a” presents IUP, “b” presents MN.

343

344 **Carbon and nitrogen isotope fractionation during photo-degradation** 345 **of IUP**

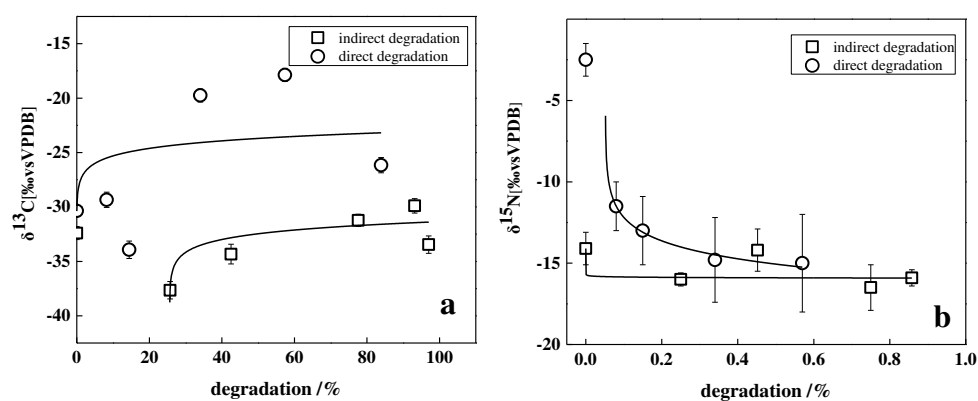
346 Compound specific isotope analysis is a valuable tool to identify such degradation
347 pathways in different environmental systems [69]. The isotope fractionation for $\delta^{13}\text{C}$
348 $\delta^{15}\text{N}$ were observed in photodegradation of IUP by direct and indirect photo-
349 degradation. The ratio of carbon isotopes ($^{13}\text{C}/^{12}\text{C}$) increased in the reactant while the
350 light isotopes (^{12}C) tended to go into reaction products, presenting a normal isotope
351 effect. In contrast, the ratio of nitrogen isotopes ($^{15}\text{N}/^{14}\text{N}$) decreased in the substrate,
352 showing an inverse isotope effect (Fig.6). The $\delta^{13}\text{C}$ values of IUP at the beginning of
353 the experiment was $-30.361 \pm 0.08\%$ and $32.3965 \pm 0.04\%$ in direct photolysis and

354 nitrate induced photo-degradation conditions, respectively. The different initial carbon
355 isotope values may be related to the initial concentration. In blank controls, the value
356 of $\delta^{13}\text{C}$ remained constant during the whole experiment (data not shown) confirming
357 that besides photodegradation no other processes lead to changes in carbon isotope
358 ratios of IUP. It worth noting that when the degradation rate was 57%, the value of $\delta^{15}\text{N}$
359 is $15.148 \pm 0.76\text{‰}$, showing obvious inverse fractionation ($\Delta=12.6615 \pm 1.2\text{‰}$);
360 However, no significant fractionation of N isotopes occurred during indirect photo-
361 degradation (Fig. 6b)

362 As shown in Fig.6, IUP photolysis resulted in a normal isotope fractionation of
363 ^{13}C , that is the substrate was enriched with the light isotopologues during the reaction.
364 The value of $\delta^{13}\text{C}$ shifts confirms that the observed fractionation was associated with
365 the direct photolysis and nitrate induced photo-degradation of IUP. Note that the
366 degradation was 15% and 57% in direct photolysis condition, the value of $\delta^{13}\text{C}$ was
367 $33.9285 \pm 0.4\text{‰}$ ($\Delta= 3.5675 \pm 0.49\text{‰}$) and $-17.8695 \pm 0.3\text{‰}$ ($\Delta=12.50 \pm 0.5\text{‰}$); While
368 the degradation was 25% and 88% with indirect photolysis, the value of $\delta^{13}\text{C}$ was 37.65
369 $\pm 0.9\text{‰}$ ($\Delta=5.2535 \pm 0.68\text{‰}$) and $-29.896 \pm 0.2\text{‰}$ ($\Delta=2.5 \pm 0.28\text{‰}$), respectively. The
370 phenomenon of inverse isotope fractionation has also appeared in the study of
371 photodegradation of other organic pollutant, which may be related to the nuclear
372 magnetic moment/nuclear spin of the isotope, rather than the isotope mass [70].
373 Hartenbac et al. [71] in the study of photolysis of atrazine, points out that the hydrolysis
374 of atrazine in normal fractional steps before other process of molecules led to such an
375 isotope effect should be (such as molecular excitation singlet and triplet can through a

376 variety of light physical process returns to the electronic ground state). Therefore, under
 377 the sunlight radiation can cause molecules in the isotope carry nuclear spin and the
 378 interaction of unpaired electrons, can produce magnetic isotope effect at this time. The
 379 result is not a light-isotope priority reaction, depending on their nuclear spin quantum
 380 number [72]. However, isotope effects associated with photophysical excitation and
 381 relaxation processes could have caused the observed isotope fractionation, but little is
 382 known that would allow one to confirm such hypotheses and requires further study [14].

383



384

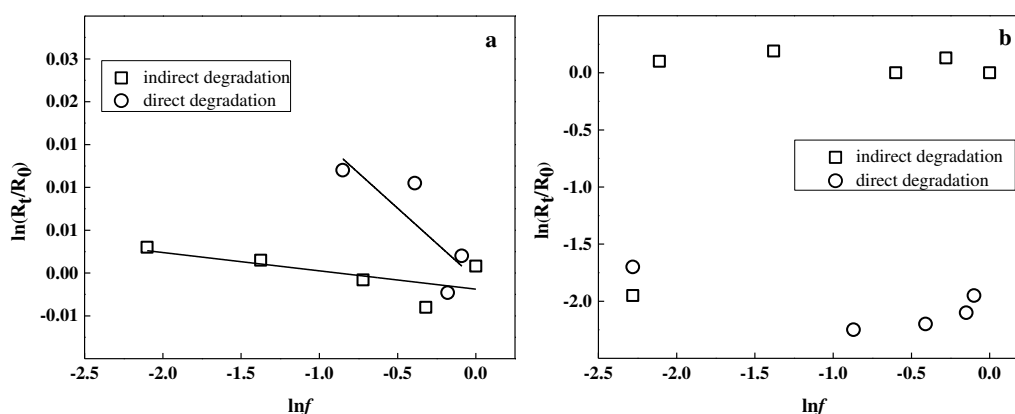
385 **Fig. 6.** Carbon (a) and nitrogen (b) isotope fractionation of IUP under different conditions.

386

387 The isotope enrichment factors for carbon was calculated according to the
 388 Rayleigh equation (eq. (2)) by a linear regression as displayed in Fig. 7a. On the
 389 contrary, nitrogen stable isotope fractionation can not be fitted well by Rayleigh
 390 equation under both photodegradation pathways, and its r^2 is less than 0.5 (Fig. 7b). It
 391 was obvious that the isotope enrichment factor for IUP is significantly different between
 392 the direct photodegradation ($\varepsilon_c = -0.018 \pm 0.006\text{‰}$) and nitrate induced
 393 photodegradation ($\varepsilon_c = -0.002 \pm 0.001\text{‰}$). The difference in the degree of stable

394 isotope fractionation between different degradation pathways is not only related to
395 specific degradation conditions (for example, the higher energy of light can break the
396 corresponding chemical bonds more quickly in the process of photodegradation), but
397 also related to the reaction mechanism of different degradation pathways [57]. It has
398 been reported that the cleavage of the bond between the carbonyl carbon and the alkyl
399 nitrogen of IPU results in primary carbon isotope effects [40]. Moreover, secondary
400 isotope effects occur at the alkyl nitrogen and the two methyl carbons, indicating that
401 the reaction of isopropyl chain does not cause carbon stable isotope fractionation, which
402 is consistent with the other reports [73].

403



404

405 **Fig. 7.** Carbon (a) and nitrogen (b) isotope enrichment factors were determined by a linear
406 regression according to the Rayleigh equation.

407

408 Conclusions

409 The direct photolysis of two organic pesticides under different light sources
410 follows first-order degradation kinetics, and the herbicides photodegradation rate
411 follows the order MN > IUP, reaching 99% degradation at 60 min of Hg lamp treatment

412 for MN and at 120 min for IUP. The irradiation time reached 18h, the MN degradation
413 rate was 78%, while the degradation rate was only 5% for IPU under the condition of
414 Xe lamp. Structural and molecular characteristics play a decisive role in these photo-
415 degradation rates. The presence of NO_3^- has a photosensitizing effect on IPU and MN,
416 and the nitrate induction can significantly affect the degradation rate of organic
417 pollutants. In indirect photodegradation, the degradation rate decreased with the
418 increase of organic substrate concentration with a certain concentration of NO_3^- . The
419 degradation rate of $\cdot\text{OH}$ on organic pesticides was independent of its functional groups
420 (IPU and MN), but related to substituents on aromatic rings. Therefore, it was suggested
421 to classify different substituents on aromatic rings of organic pesticides, so as to further
422 obtain the photodegradation law of different organic pesticides. According to the
423 isotope fractionation, photolysis of IUP exhibits normal carbon isotope fractionation
424 with the degradation rate increases, and the stable isotope enrichment factors under
425 different photolysis pathways are different. In the indirect photodegradation process,
426 no significant fractionation of nitrogen isotopes occurred, and stable nitrogen isotopes
427 fractionation could not be fitted well in either of the two photodegradation pathways.
428 These results are useful for evaluating the environmental fate of phenylurea herbicides
429 as well as other organic pollutants.

430

431 **Abbreviations**

432 IUP: isopropiron; MN: methylamine; CSIA: compound-specific isotope analysis; UV:
433 ultraviolet; $\delta^{13}\text{C}$: carbon stable isotope; $\delta^{15}\text{N}$: nitrogen stable isotope; C: carbon; N:

434 nitrogen; VPDB: Vienna Pee Dee Belemnite; $^{13}\text{C}/^{12}\text{C}$: carbon isotopes ratio; $^{15}\text{N}/^{14}\text{N}$:
435 nitrogen isotopes ratio.

436 **Ethics approval and consent to participate**

437 Not applicable.

438 **Consent for publication**

439 Not applicable.

440 **Availability of data and materials**

441 The data sets supporting the conclusions of this article are included within the article.

442 **Competing interests**

443 The authors declare that they have no competing interests.

444 **Funding**

445 This work was supported by the National Key R&D Program of China
446 (2018YFC1803100) and National Natural Science Foundation of China (No.
447 21377098).

448 **Authors' contributions**

449 Haiyan Yu, Jinling Liu, Changxu Han, Han Fang, Xingquan Shu, and Yongfeng Liu
450 performed the experiments. Haiyan Yu wrote the manuscript. Limin Ma and Yuwei Pan
451 contributed to the manuscript correction. All authors read and approved the final
452 manuscript.

453 **Acknowledgements**

454 The valuable comments of Professor Limin Ma are acknowledged.

455

456 **References**

- 457 1. Mestankova, H.; Escher, B.; Schirmer, K.; von Gunten, U.; Canonica, S., 2011. Evolution of
458 algal toxicity during (photo)oxidative degradation of diuron. *Aquatic Toxicology*, 101, (2),
459 466-473.
- 460 2. Tilman, D., Cassman, K.G., Matson, P.A., Naylor, R., Polasky, S., 2002. Agricultural
461 sustainability and intensive production practices, *Nature*, 418(6898), 671-7.
- 462 3. Zhao, Q.; Hu, H. B.; Wang, W.; Huang, X. Q.; Zhang, X. H., 2017. Novel Three-Component
463 Phenazine-1-Carboxylic Acid 1,2-Dioxygenase in *Sphingomonas wittichii* DP58. *Appl*

- 464 Environ Microbiol, 83, (9).
- 465 4. Huasong, P.; Qingwen, H.; Bilal, M.; Wang, W.; Zhang, X., 2018. Kinetics, mechanism, and
466 identification of photodegradation products of phenazine-1-carboxylic acid. Environmental
467 Technology, 1-9.
- 468 5. Orellana-García, F.; Álvarez, M. A.; López-Ramón, V.; Rivera-Utrilla, J.; Sánchez-Polo, M.;
469 Mota, A. J., 2014. Photodegradation of herbicides with different chemical natures in aqueous
470 solution by ultraviolet radiation. Effects of operational variables and solution chemistry.
471 Chemical Engineering Journal, 255, 307-315.
- 472 6. Chen, X.M., Wang, C.L., Bo, R., 2016. Current situation of Chinese pesticide application and
473 policy suggestions. Pesticide science and administration, 37(2),4-8.
- 474 7. Farre, M. J.; Domenech, X.; Peral, J., 2007. Combined photo-Fenton and biological treatment
475 for Diuron and Linuron removal from water containing humic acid. J Hazard Mater, 147, (1-
476 2), 167-74.
- 477 8. Hernández, F.; Sancho, J. V.; Pozo, O. J., 2005. Critical review of the application of liquid
478 chromatography/mass spectrometry to the determination of pesticide residues in biological
479 samples. Analytical and Bioanalytical Chemistry, 382, (4), 934-946.
- 480 9. Zhao, Q.; Yue, S.; Bilal, M.; Hu, H.; Wang, W.; Zhang, X., 2017. Comparative genomic
481 analysis of 26 Sphingomonas and Sphingobium strains: Dissemination of bioremediation
482 capabilities, biodegradation potential and horizontal gene transfer. Science of The Total
483 Environment, 609, 1238-1247.
- 484 10. Álvarez', P. M.; Beltrán, F. J.; Masa, F. J.; Pocostales, J. P., 2009. A comparison between
485 catalytic ozonation and activated carbon adsorption/ozone-regeneration processes for
486 wastewater treatment. Applied Catalysis B: Environmental, 92, (3-4), 393-400.
- 487 11. Tan, C.; Gao, N.; Deng, Y.; An, N.; Deng, J., 2012. Heat-activated persulfate oxidation of
488 diuron in water. Chemical Engineering Journal, 203, 294-300.
- 489 12. Oturan, M. A.; Oturan, N.; Edelahi, M. C.; Podvorica, F. I.; Kacemi, K. E., 2011. Oxidative
490 degradation of herbicide diuron in aqueous medium by Fenton's reaction based advanced
491 oxidation processes. Chemical Engineering Journal, 171, (1), 127-135.
- 492 13. Fenner, K., Canonica, S., Wackett, L.P., Elsner, M., 2013. Evaluating Pesticide Degradation in
493 the Environment_ Blind Spots and Emerging Opportunities. Science, 41, 752-758.
- 494 14. Hartenbach, A.E., Hofstetter, T.B., Tentscher, P.R., Canonica, S., Berg, M., Schwarzenbach,
495 R.P., 2008. Carbon, Hydrogen, and Nitrogen Isotope Fractionation During Light-Induced
496 Transformations of Atrazine, Environmental Science & Technology 42, 7751-7756.
- 497 15. Burrows, H.D., Canle, M., Santaballa, J.A., Steenken, S., 2002. Reaction pathways and
498 mechanisms of photodegradation of pesticides. Journal of photochemistry and photobiology b-
499 biology. 67, 71-108.
- 500 16. Chen, J.W., Quan, X., Peijnenburg, W.J.G.M., Yang, F.L., 2001. Quantitative structure-property
501 relationships (QSPRs) on direct photolysis of PCDDs. Chemosphere, 43, 235-241.
- 502 17. Niu, J.; Chen, J.; Martens, D.; Henkelmann, B.; Quan, X.; Yang, F.; Seidlitz, H. K.; Schramm,
503 K. W., 2004. The role of UV-B on the degradation of PCDD/Fs and PAHs sorbed on surfaces
504 of spruce (*Picea abies* (L.) Karst.) needles. Sci Total Environ, 322, (1-3), 231-41.
- 505 18. Barlow, N. J.; Phillips, S. L.; Wallace, D. G.; Sar, M.; Gaido, K. W.; Foster, P. M., 2003.
506 Quantitative changes in gene expression in fetal rat testes following exposure to di(n-butyl)
507 phthalate. Toxicol Sci, 73, (2), 431-41.

- 508 19. Hijnen, W. A. M.; Beerendonk, E. F.; Medema, G. J., 2006. Inactivation credit of UV radiation
509 for viruses, bacteria and protozoan (oo)cysts in water: A review. *Water Research*, 40, (1), 3-22.
- 510 20. Lazarova, V., Savoye, P., 2004. Technical and sanitary aspects of wastewater disinfection by
511 UV irradiation for landscape irrigation. *Water Science and Technology*, 50, 203-209.
- 512 21. Sanches, S.; Barreto Crespo, M. T.; Pereira, V. J., 2010. Drinking water treatment of priority
513 pesticides using low pressure UV photolysis and advanced oxidation processes. *Water
514 Research*, 44, (6), 1809-1818.
- 515 22. Chen, C.; Yang, S.; Guo, Y.; Sun, C.; Gu, C.; Xu, B., 2009. Photolytic destruction of endocrine
516 disruptor atrazine in aqueous solution under UV irradiation: Products and pathways. *Journal
517 of Hazardous Materials*, 172, (2-3), 675-684.
- 518 23. Prados-Joya, G.; Sánchez-Polo, M.; Rivera-Utrilla, J.; Ferro-garcía, M., 2011.
519 Photodegradation of the antibiotics nitroimidazoles in aqueous solution by ultraviolet radiation.
520 *Water Research*, 45, (1), 393-403.
- 521 24. Rosas, J. M.; Vicente, F.; Saguillo, E. G.; Santos, A.; Romero, A., 2014. Remediation of soil
522 polluted with herbicides by Fenton-like reaction: Kinetic model of diuron degradation. *Applied
523 Catalysis B: Environmental*, 144, 252-260.
- 524 25. Hessler, D.P., Gorenflo, V., Frimmel, F.H., 1993. Degradation of Aqueous Atrazine and
525 Metazachlor Solutions by UV and UV/H₂O₂-Influence of pH and Herbicide
526 Concentration. *Acta hydrochimica et hydrobiologica*, 21(4):209-214.
- 527 26. Latch, D.E., Stender, B.L., Packer, J.L., Arnold, W.A., McNeill, K., 2003. Photochemical Fate
528 of Pharmaceuticals in the Environment: Cimetidine and Ranitidine. *Environmental Science
529 & Technology*, 37(15), 3342-3350.
- 530 27. Packer, J. L.; Werner, J. J.; Latch, D. E.; McNeill, K.; Arnold, W. A., 2003. Photochemical fate
531 of pharmaceuticals in the environment: Naproxen, diclofenac, clofibric acid, and ibuprofen.
532 *Aquatic Sciences - Research Across Boundaries*, 65, (4), 342-351.
- 533 28. Carbonaro, S.; Sugihara, M. N.; Strathmann, T. J., 2013. Continuous-flow photocatalytic
534 treatment of pharmaceutical micropollutants: Activity, inhibition, and deactivation of TiO₂
535 photocatalysts in wastewater effluent. *Applied Catalysis B: Environmental*, 129, 1-12.
- 536 29. Choina, J.; Kosslick, H.; Fischer, C.; Flechsig, G. U.; Frunza, L.; Schulz, A., 2013.
537 Photocatalytic decomposition of pharmaceutical ibuprofen pollutions in water over titania
538 catalyst. *Applied Catalysis B: Environmental*, 129, 589-598.
- 539 30. Martinez, F.; Lopez-Munoz, M. J.; Aguado, J.; Melero, J. A.; Arsuaga, J.; Sotto, A.; Molina,
540 R.; Segura, Y.; Pariente, M. I.; Revilla, A.; Cerro, L.; Carenas, G., 2013. Coupling membrane
541 separation and photocatalytic oxidation processes for the degradation of pharmaceutical
542 pollutants. *Water Res*, 47, (15), 5647-58.
- 543 31. Měšt'ánková, H.; Krýsa, J.; Jirkovský, J.; Mailhot, G.; Bolte, M., 2005. The influence of Fe(III)
544 speciation on supported TiO₂ efficiency: example of monuron photocatalytic degradation.
545 *Applied Catalysis B: Environmental*, 58, (3-4), 185-191.
- 546 32. Oturan, M. A.; Edelahe, M. C.; Oturan, N.; El kacemi, K.; Aaron, J.-J., 2010. Kinetics of
547 oxidative degradation/mineralization pathways of the phenylurea herbicides diuron, monuron
548 and fenuron in water during application of the electro-Fenton process. *Applied Catalysis B:
549 Environmental*, 97, (1-2), 82-89.
- 550 33. Mest'ankova, H.; Mailhot, G.; Pilichowski, J. F.; Krysa, J.; Jirkovsky, J.; Bolte, M., 2004.
551 Mineralisation of Monuron photoinduced by Fe (III) in aqueous solution. *Chemosphere*, 57,

- 552 (10), 1307-15.
- 553 34. Bobu, M.; Wilson, S.; Greibrokk, T.; Lundanes, E.; Siminiceanu, I., 2006. Comparison of
554 advanced oxidation processes and identification of monuron photodegradation products in
555 aqueous solution. *Chemosphere*, 63, (10), 1718-27.
- 556 35. Shankar, M. V.; Nelieu, S.; Kerhoas, L.; Einhorn, J., 2008. Natural sunlight $\text{NO}_3^-/\text{NO}_2^-$ induced
557 photo-degradation of phenylurea herbicides in water. *Chemosphere*, 71, (8), 1461-8.
- 558 36. Nelieu, S.; Kerhoas, L.; Sarakha, M.; Einhorn, J., 2004. Nitrite and nitrate induced
559 photodegradation of monolinuron in aqueous solution. *Environmental Chemistry Letters*, 2,
560 (2),83-87.
- 561 37. Mack, J., Bolton, J.R.,1999. Photochemistry of nitrite and nitrate in aqueous solution:a review.
562 128(1-3),1-13.
- 563 38. Warneck, P., Wurzinger, C., 1988. Product quantum yields for the 305 nm photodecomposition
564 of NO_3^- in aqueous solution. *Journal of Physical Chemistry*, 92(22),6278-6283.
- 565 39. Boucheloukh, H.; Sehili, T.; Kouachi, N.; Djebbar, K., 2012. Kinetic and analytical study of
566 the photo-induced degradation of monuron by nitrates and nitrites under irradiation or in the
567 dark. *Photochem Photobiol Sci*, 11, (8), 1339-45.
- 568 40. Jin, B.; Rolle, M., 2016. Position-specific isotope modeling of organic micropollutants
569 transformation through different reaction pathways. *Environ Pollut*, 210, 94-103.
- 570 41. Nélieu, S.; Shankar, M. V.; Kerhoas, L.; Einhorn, J., 2008. Phototransformation of monuron
571 induced by nitrate and nitrite ions in water: Contribution of photonitration. *Journal of*
572 *Photochemistry and Photobiology A: Chemistry*, 193, (1), 1-9.
- 573 42. Catastini, C.; Rafqah, S.; Mailhot, G.; Sarakha, M., 2004. Degradation of amitrole by excitation
574 of iron (III) aquacomplexes in aqueous solutions. *Journal of Photochemistry and Photobiology*
575 *A: Chemistry*, 162, (1), 97-103.
- 576 43. Durst, R.; Imfeld, G.; Lange, J., 2013. Transport of pesticides and artificial tracers in vertical-
577 flow lab-scale wetlands. *Water Resources Research*, 49, (1), 554-564.
- 578 44. Imfeld, G.; Lefrancq, M.; Maillard, E.; Payraudeau, S., 2013. Transport and attenuation of
579 dissolved glyphosate and AMPA in a stormwater wetland. *Chemosphere*, 90, (4), 1333-1339.
- 580 45. Pal, A.; Gin, K. Y.-H.; Lin, A. Y.-C.; Reinhard, M., 2010. Impacts of emerging organic
581 contaminants on freshwater resources: Review of recent occurrences, sources, fate and effects.
582 *Science of The Total Environment*, 408, (24), 6062-6069.
- 583 46. Wu, L.; Liu, Y.; Liu, X.; Bajaj, A.; Sharma, M.; Lal, R.; Richnow, H. H., 2019. Isotope
584 fractionation approach to characterize the reactive transport processes governing the fate of
585 hexachlorocyclohexanes at a contaminated site in India. *Environ Int*, 132, 105036.
- 586 47. Harrington, R.R., Poulson, S.R., Drever, J.I., Colberg, P.J.S., Kelly, E.F.,1999. Carbon isotope
587 systematics of monoaromatic hydrocarbons_ vaporization and adsorption experiments.
588 *Organic geochemistry*,30 (8A),765-775.
- 589 48. Peng, X.; Li, X.; Feng, L., 2013. Behavior of stable carbon isotope of phthalate acid esters
590 during photolysis under ultraviolet irradiation. *Chemosphere*, 92, (11), 1557-62.
- 591 49. Meyer, A. H.; Elsner, M., 2013. $^{13}\text{C}/^{12}\text{C}$ and $^{15}\text{N}/^{14}\text{N}$ isotope analysis to characterize
592 degradation of atrazine: evidence from parent and daughter compound values. *Environ Sci*
593 *Technol*, 47, (13), 6884-91.
- 594 50. Maier, M. P.; De Corte, S.; Nitsche, S.; Spaett, T.; Boon, N.; Elsner, M., 2014. C & N isotope
595 analysis of diclofenac to distinguish oxidative and reductive transformation and to track

- 596 commercial products. *Environ Sci Technol*, 48, (4), 2312-20.
- 597 51. Penning, H., Sorensen, S.R., Meyer, A.H., Aamand, J., Elsner, M., 2010. C, N, and H Isotope
598 Fractionation of the Herbicide Isoproturon Reflects Different Microbial Transformation
599 Pathways. *Environmental Science & Technology*, 44(7), 2372-2378.
- 600 52. Meyer, A.H., Penning, H., Lowag, H., Elsner, M., 2008. Precise and accurate com-
601 pound specific carbon and nitrogen isotope analysis of atrazine:critical role of combustion oven
602 conditions. *Environmental Science & Technology*, 42(21),7757-7763.
- 603 53. Elsner, M.; Jochmann, M. A.; Hofstetter, T. B.; Hunkeler, D.; Bernstein, A.; Schmidt, T. C.;
604 Schimmelmann, A., 2012. Current challenges in compound-specific stable isotope analysis of
605 environmental organic contaminants. *Analytical and Bioanalytical Chemistry*, 403, (9), 2471-
606 2491.
- 607 54. Hofstetter, T. B.; Berg, M., 2011. Assessing transformation processes of organic contaminants
608 by compound-specific stable isotope analysis. *TrAC Trends in Analytical Chemistry*, 30, (4),
609 618-627.
- 610 55. Thullner, M.; Centler, F.; Richnow, H.-H.; Fischer, A., 2012. Quantification of organic
611 pollutant degradation in contaminated aquifers using compound specific stable isotope analysis
612 – Review of recent developments. *Organic Geochemistry*, 42, (12), 1440-1460.
- 613 56. Hirschorn, S.K., Dinglasan, M.J., Elsner, M., Mancini, S.A., Lacrampe-Couloume, G.,
614 Edwards, E.A., Lollar, B.S., 2004. Pathway dependent isotopic fractionation during aerobic
615 biodegradation of 1,2-dichloroethane. *Environmental Science & Technology*, 38(18), 4775-
616 4781.
- 617 57. Zwank, L., Berg, M., Elsner, M., Schmidt, T.C., Schwarzenbach, R.P., Haderlein, S.B., 2005.
618 New evaluation scheme for two-dimensional isotope analysis to decipher biodegradation
619 processes:Application to groundwater contamination by MTBE. *Environmental Science &
620 Technology*, 39(4), 1018-1029.
- 621 58. Elsner, M., Zwank, L., Hunkeler, D., Schwarzenbach, R.P., 2005. A new concept linking
622 observable stable isotope fractionation to transformation pathways of organic pollutants.
623 *Environmental Science & Technology*, 39(18), 6896-6916.
- 624 59. Meyer, A.H., Penning, H., Elsner, M., 2009. C and N Isotope Fractionation Suggests Similar
625 Mechanisms of Microbial Atrazine Transformation Despite Involvement of Different Enzymes
626 (AtzA and TrzN). *Environmental Science & Technology*, 43(21), 8079-8085.
- 627 60. Coplen, T. B., 2011. Guidelines and recommended terms for expression of stable-isotope-ratio
628 and gas-ratio measurement results. *Rapid Communications in Mass Spectrometry*, 25, (17),
629 2538-2560.
- 630 61. Abe, Y., Hunkeler, D., 2006. Does the Rayleigh Equation Apply to Evaluate Field Isotope Data
631 in Contaminant Hydrogeology. *Environmental Science & Technology*, 40(5), 1588-1596.
- 632 62. Zhou, Y.; Zhao, J.; Zhang, Y. N.; Qu, J.; Li, C.; Qin, W.; Zhao, Y.; Chen, J.; Peijnenburg, W.,
633 2019. Trace amounts of fenofibrate acid sensitize the photodegradation of bezafibrate in
634 effluents: Mechanisms, degradation pathways, and toxicity evaluation. *Chemosphere*, 235,
635 900-907.
- 636 63. Tian, Q., Zhou, Z.Q., Ren, L.P., Jiang, S.R., Yang, L., 2005. Research Development of
637 Pesticides Photodegradation in Water. *Chinese Journal of Pesticides*,44(6),247-250.
- 638 64. Shen, J.L., Ji, M.S., Tian, H.Z., 2015. Research progress of pesticides chemical degradation in
639 water. *Agrochemicals*,54(4):248-250.

- 640 65. Ta, N.; Hong, J.; Liu, T.; Sun, C., 2006. Degradation of atrazine by microwave-assisted
641 electrodeless discharge mercury lamp in aqueous solution. *J Hazard Mater*, 138, (1), 187-94.
- 642 66. Arantegui, J., Prado, J., Chamarro, E., Esplugas, S., 1995. Kinetics of the UV degradation of
643 atrazine in aqueous solution in the presence of hydrogen peroxide. *Journal of photochemistry
644 and photobiology A-chemical*, 88(1), 65-74.
- 645 67. Xu, P.J., Liu, H., Zhou, Z.H., Xu, W.T., 2011. Study on ultraviolet photodegradation of p-
646 nitrobenzoic acid with nitrate. *Chinese Journal of Environmental Engineering*, 5(1), 80-84.
- 647 68. Canle López, M.; Fernández, M. I.; Rodríguez, S.; Santaballa, J. A.; Steenken, S.; Vulliet, E.,
648 2005. Mechanisms of Direct and TiO₂-Photocatalysed UV Degradation of Phenylurea
649 Herbicides. *Chem Phys Chem*, 6, (10), 2064-2074.
- 650 69. Elsner, M., 2010. Stable isotope fractionation to investigate natural transformation mechanisms
651 of organic contaminants: principles, prospects and limitations. *J Environ Monit*, 12, (11), 2005-
652 31.
- 653 70. Buchachenko, A. L., 2013. Mass-independent isotope effects. *J Phys Chem B*, 117, (8), 2231-
654 8.
- 655 71. Hartenbach, A.E., Hofstetter, T.B., Tentscher, P.R., Canonica, S., Berg, M., Schwarzenbach,
656 R.P., 2008. Carbon, hydrogen, and nitrogen isotope fractionation during light-induced
657 transformations of atrazine. *Environmental Science & Technology*, 42(21), 7751-7756.
- 658 72. Buchachenko, A.L., Ivanov, V.L., Roznyatovsky, V.A., Ustynyuk, Y.A., 2006. Magnetic
659 isotope effect in the photolysis of organotin compounds. *Journal of Physical Chemistry A*,
660 110(11), 3857-3859.
- 661 73. Penning, H., Elsner, M., 2007. Intramolecular carbon and nitrogen isotope analysis by
662 quantitative dry fragmentation of the phenylurea herbicide isoproturon in a combined injector
663 capillary reactor prior to GC separation. *Analytical chemistry*, 79(21), 8399-8405.

664

Figures

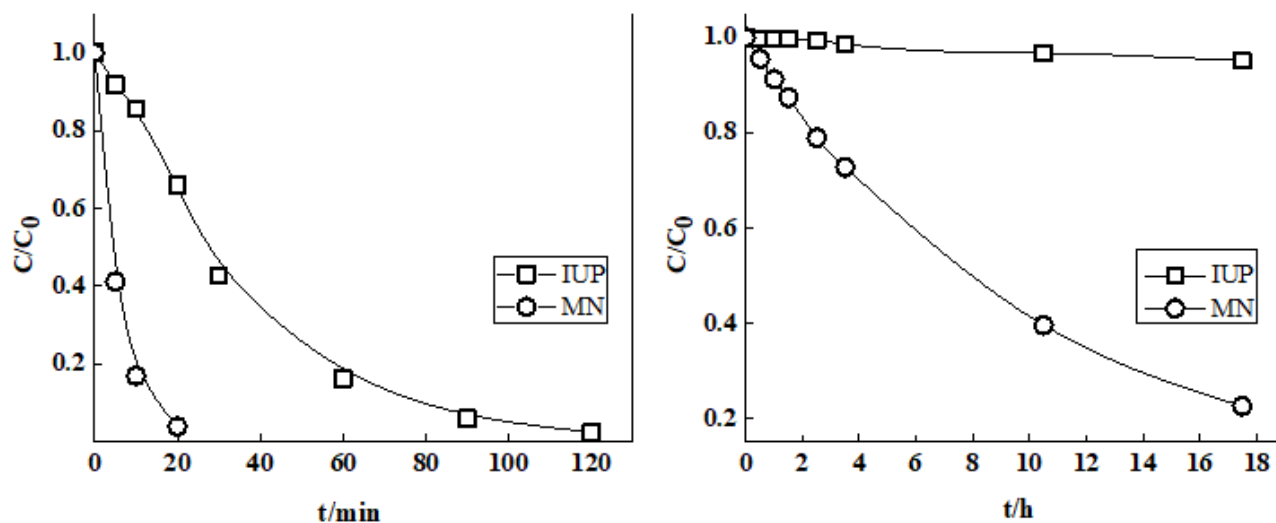


Figure 1

Removal kinetics of herbicides by ultraviolet photodegradation. Notes: "a" presents Hg lamp, "b" presents Xe lamp.

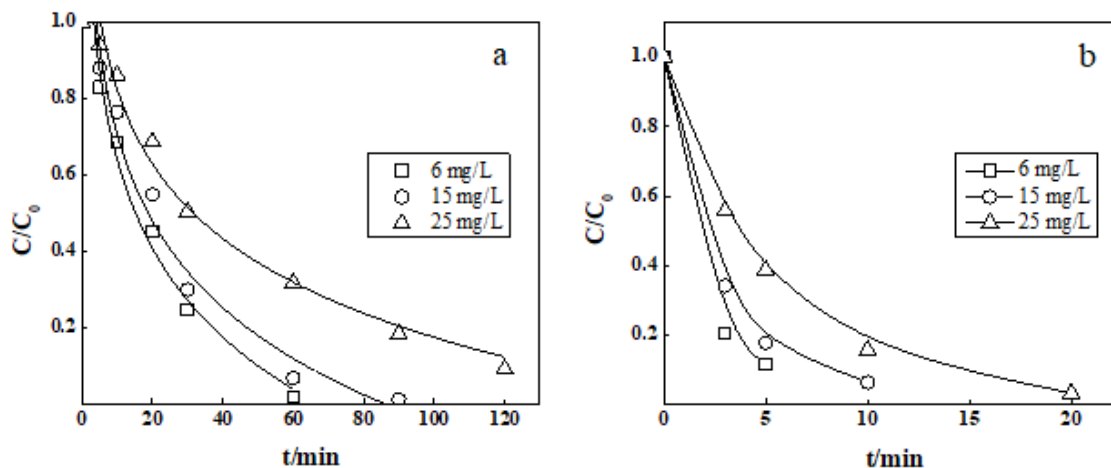


Figure 2

Influence of the initial concentration of herbicides on the photodegradation. Notes: "a" presents IUP, "b" presents MN.

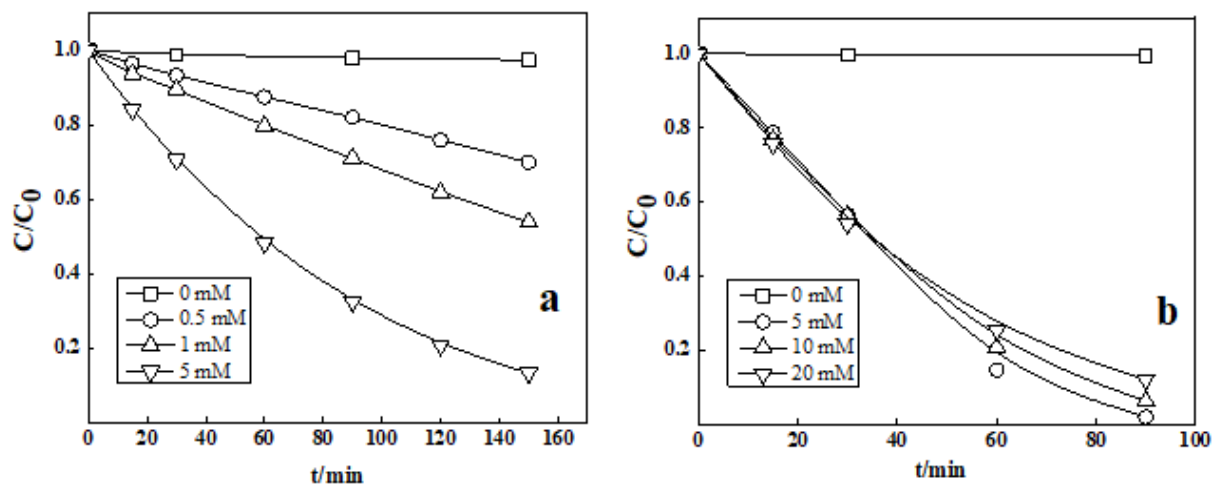


Figure 3

Influence of the nitrate concentration on the photodegradation of IUP by UV radiation. Notes: "a" presents substrate concentration is 8 mg/L, "b" presents substrate concentration is 30 mg/L.

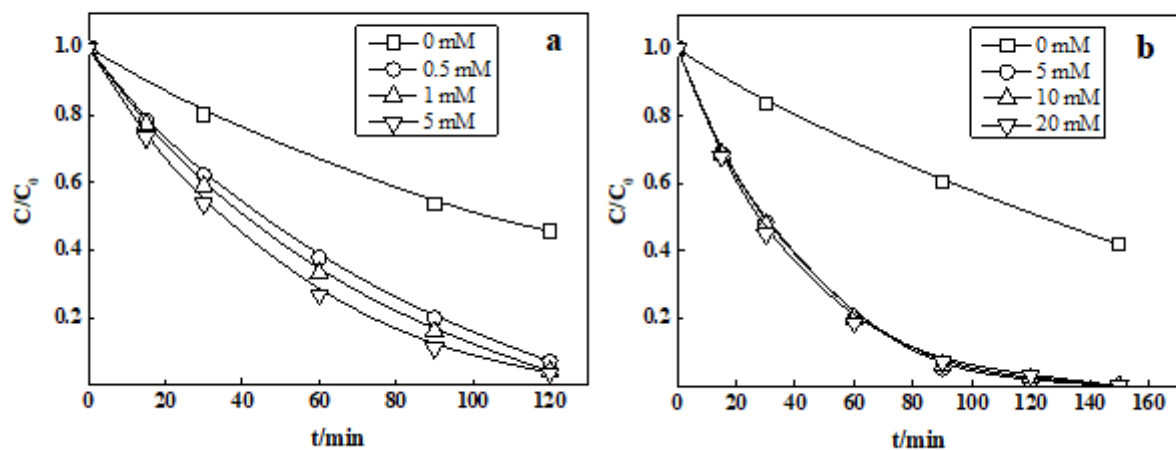


Figure 4

Influence of the nitrate concentration on the photodegradation of MN by UV radiation. Notes: "a" presents the substrate concentration is 8 mg/L, "b" presents the substrate concentration is 30 mg/L.

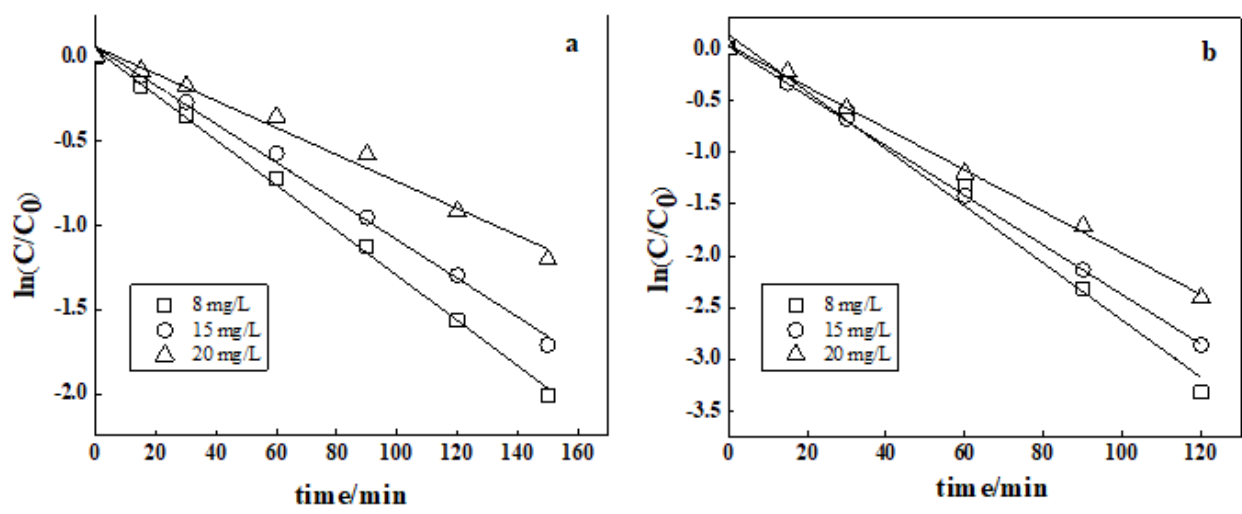


Figure 5
 Influence of the substrate concentration on the photodegradation in the presence of NO_3^- (5 mM). Notes: "a" presents IUP, "b" presents MN.

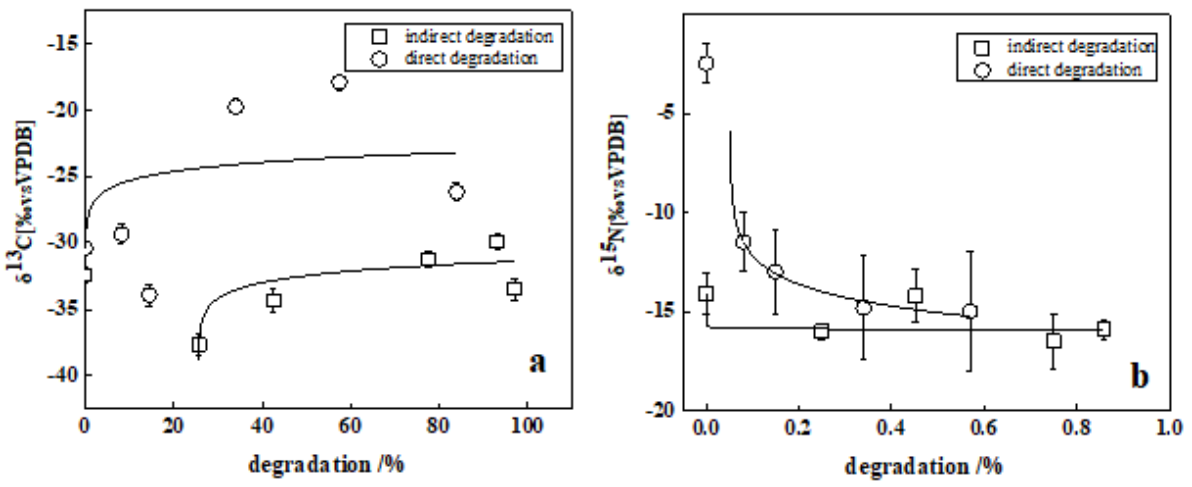


Figure 6
 Carbon (a) and nitrogen (b) isotope fractionation of IUP under different conditions.

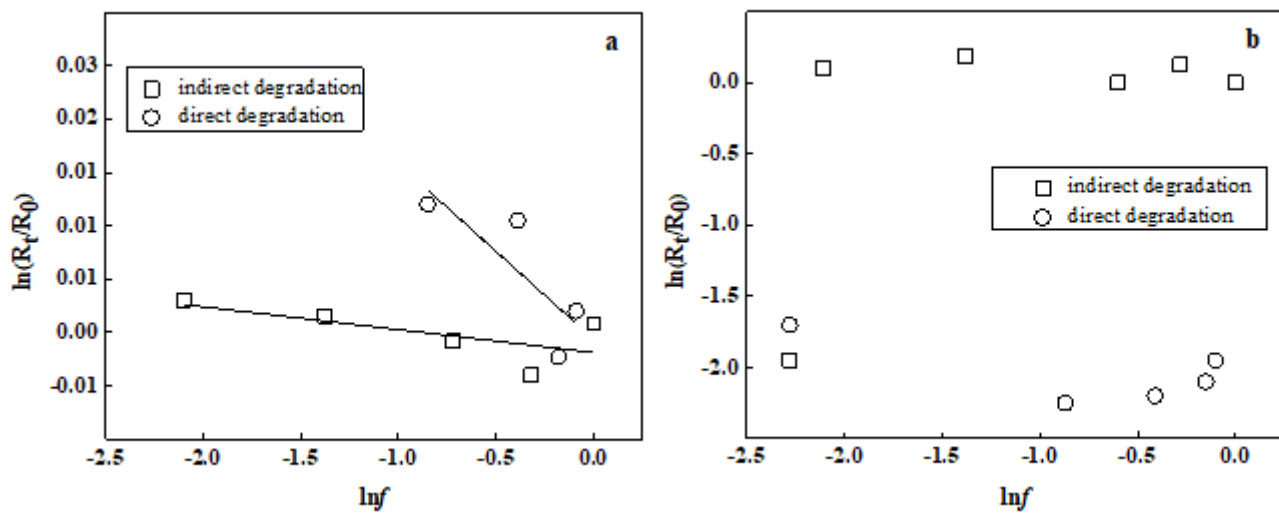


Figure 7

Carbon (a) and nitrogen (b) isotope enrichment factors were determined by a linear regression according to the Rayleigh equation.

Supplementary Files

This is a list of supplementary files associated with this preprint. Click to download.

- [SupplementaryMaterial12.28.docx](#)